UNIVERSITY OF WEST LONDON
The Career University

UWL REPOSITORY

repository.uwl.ac.uk

Effect of high-intensity ultrasonic treatment on the physicochemical, structural, rheological, behavioral, and foaming properties of pumpkin (Cucurbita moschata Duch.)-seed protein isolates

Du, Hongying, Zhang, Jin, Wang, Siqi, Manyande, Anne ORCID logoORCID: https://orcid.org/0000-0002-8257-0722 and Wang, Jie (2022) Effect of high-intensity ultrasonic treatment on the physicochemical, structural, rheological, behavioral, and foaming properties of pumpkin (Cucurbita moschata Duch.)-seed protein isolates. LWT, 155. p. 112952. ISSN 0023-6438

http://dx.doi.org/10.1016/j.lwt.2021.112952

This is the Published Version of the final output.

UWL repository link: https://repository.uwl.ac.uk/id/eprint/8735/

Alternative formats: If you require this document in an alternative format, please contact: open.research@uwl.ac.uk

Copyright: Creative Commons: Attribution-Noncommercial-No Derivative Works 4.0

Copyright and moral rights for the publications made accessible in the public portal are retained by the authors and/or other copyright owners and it is a condition of accessing publications that users recognise and abide by the legal requirements associated with these rights.

Take down policy: If you believe that this document breaches copyright, please contact us at open.research@uwl.ac.uk providing details, and we will remove access to the work immediately and investigate your claim.

LWT - Food Science and Technology 155 (2022) 112952

Contents lists available at ScienceDirect

LWT

journal homepage: www.elsevier.com/locate/lwt

Effect of high-intensity ultrasonic treatment on the physicochemical, structural, rheological, behavioral, and foaming properties of pumpkin (*Cucurbita moschata* Duch.)-seed protein isolates

Hongying Du [a,c], Jin Zhang [b], Siqi Wang [a], Anne Manyande [d], Jie Wang [e,f,*]

[a] Key Laboratory of Environment Correlative Dietology, Ministry of Education, College of Food Science and Technology, Huazhong Agricultural University, Wuhan, 430070, Hubei, PR China
[b] Institute of Food Science, Zhejiang-Russia Joint R & D Center for Nutritional and Health Food Green Manufacturing, Zhejiang Academy of Agricultural Sciences, Hangzhou, 310021, Zhejiang, PR China
[c] National R & D Branch Center for Conventional Freshwater Fish Processing, Wuhan, 430070, Hubei, PR China
[d] School of Human and Social Sciences, University of West London, London, UK
[e] Key Laboratory of Magnetic Resonance in Biological Systems, State Key Laboratory of Magnetic Resonance and Atomic and Molecular Physics, National Center for Magnetic Resonance in Wuhan, Wuhan Institute of Physics and Mathematics, Innovation Academy for Precision Measurement Science and Technology, Chinese Academy of Sciences-Wuhan National Laboratory for Optoelectronics, 430071, Wuhan, People's Republic of China
[f] University of Chinese Academy of Sciences, Beijing, 100049, PR China

ARTICLE INFO

Keywords:
High-intensity ultrasound
Pumpkin-seed protein
Structural characteristics

ABSTRACT

Pumpkin-seed protein isolates were treated with high-intensity ultrasound (HIU). The effects of different ultrasound powers at the same treating time on the physicochemical, structure and foaming properties of pumpkin-seed protein isolates (PSPIs) were investigated. The results showed that the ultrasound treatment transformed the PSPI aggregates into smaller aggregates with a more uniform distribution. When the pH value increased, the solubility and foaming ability of the protein also increased significantly. Increasing the ultrasound power also increased the surface hydrophobicity of the PSPIs and the total sulfhydryl contents, while the active sulfhydryl content decreased. The most significant effect on the total sulfhydryl content occurred when 500 W ultrasonic power was used. The ultrasound treatment also had a significant effect on the chromaticity and turbidity of the pumpkin-seed protein isolates. With an increase in ultrasonic power, scanning electron microscopy (SEM) showed that the sizes of particles decreased as their distribution increased. Moreover, ultrasound treatment was found to be beneficial for enhancing and improving foaming performance. Ultrasound modification affected the protein's physicochemical properties and structure, which contributed greatly to the corresponding functional and nutritional properties of the protein. It would be, therefore, useful to develop and utilize plant protein and to improve its added-value.

1. Introduction

Pumpkin (*Cucurbita moschata* Duch., Cucurbitaceae) is a common plant that grows in tropical, subtropical, and warm regions around the world and is used in the food industry for the production of purees, juices, jams, and alcoholic beverages (Mitić et al., 2018). Pumpkin seeds, a food oil crop, are utilized widely in the production of vegetable oils due to their high nutritional value and health-promoting effects (Aktaş et al., 2018). Due to increases in pumpkin-seed oil production, a large quantity of pumpkin-seed cake is produced as a by-product and often used as livestock feed (*3*). In recent years, pumpkin seed cake has attracted much attention because of its high protein content (60–65%) and the special functional characteristics of its plant proteins. Furthermore, the main fraction of pumpkin-seed proteins is 12S globulin, in which the structure is similar to that of globulins in legume seeds (Bučko et al., 2015). This similarity indicates that pumpkin-seed protein isolate (PSPI) has comparative functional properties to legume seed proteins, such as emulsifying, foaming, and gelling abilities (Yang et al., 2019). Therefore, PSPI should be extracted and transferred to value-added products as functional ingredients and nutritional additives in the food

* Corresponding author. Key Laboratory of Environment Correlative Dietology, Ministry of Education, College of Food Science and Technology, Huazhong Agricultural University, Wuhan, 430070, Hubei, PR China.
E-mail address: jie.wang@wipm.ac.cn (J. Wang).

https://doi.org/10.1016/j.lwt.2021.112952
Received 9 August 2021; Received in revised form 28 October 2021; Accepted 7 December 2021
Available online 9 December 2021
0023-6438/© 2021 The Authors. Published by Elsevier Ltd. This is an open access article under the CC BY-NC-ND license (http://creativecommons.org/licenses/by-nc-nd/4.0/).

industry.

Ultrasound is a promising green technology with a low impact on the environment and has been widely used for food processing and extracting bioactive substances from plant, animal, and marine sources (Chemat et al., 2011; Ojha et al., 2020). Notably, ultrasound has been used as an alternative for changing or improving the functional properties of various proteins. For instance, ultrasound-treated chicken myofibrillar protein presented better emulsifying, rheological, and stability properties (Wang et al., 2020). Ultrasound treatment modified the physical–chemical, functional, and structural properties of canola protein isolate (Flores-Jiménez et al., 2019). Moreover, the antioxidant activity of watermelon seed protein improved, and the protein structure changed, after divergent ultrasound pretreatment (Wen et al., 2019). Furthermore, with a combination of ultrasound treatment and kluyveromyces marxianus fermentation, the antigenicity of bovine whey proteins was reduced significantly (Zhao et al., 2020). Some products based on soy proteins and whey involved in industrial production are processed with ultrasound to produce different forms of creams, pastes, and other substances (Téllez-Morales et al., 2020). Therefore, ultrasonic treatment is currently considered to be a powerful tool in the protein processing industries and other related fields.

There are many reports on how treatment with ultrasound enhanced the processing applicability and functional properties of proteins, such as in fava beans (Martínez-Velasco et al., 2018), sunflower (Malik & Saini, 2018), rice (Zhang et al., 2018), chicken (Zou et al., 2018), canola (Flores-Jiménez et al., 2019), and album seed protein isolates (Mir et al., 2019). However, few studies have focused on the physiochemical properties and functions of pumpkin-seed protein isolate, including the solubility, interface, adsorption, emulsifying, foaming, antioxidative activities, and changes after enzymatic hydrolysis (Bučko et al., 2015, 2016, 2018; Nkosi et al., 2006; Quirino et al., 2014). To our best knowledge, there are no reports on the effects of ultrasounds on improving the quality of PSPI as a food ingredient in industry. Therefore, the aim of the present study was to determine the physicochemical, functional, foaming, and structural properties of PSPI as indicators of its potential use in the food industry.

2. Material and methods

2.1. Materials

Fresh pumpkins (*C. moschata* Duch.) were purchased from a local market of Huazhong Agricultural University (Wuhan, Hubei, China). The pumpkin seed powders (PSD) were prepared from pumpkins through cutting, cleaning, and drying. The contents of moisture, fat, protein, and other nutrients of the obtained PSD were 4.95 ± 0.04%, 35.59 ± 1.12%, 19.63 ± 0.216%, and 39.83 ± 1.38%, respectively, based on the official AOAC (Association of Official Analytical Chemists) methods of analysis. The water used in the present study was deionized (DI) and all the chemicals used were of analytical grade.

2.2. Preparation of pumpkin-seed protein isolate

Pumpkin-seed protein isolate (PSPI) were prepared from pumpkin-seed powder using alkali extraction with isoelectric precipitation, as described by Bučko et al. (Bučko et al., 2015) with little modification. Briefly, pumpkin-seed protein powder was defatted for 4 h using hexane in a Soxhlet extraction apparatus. The defatted pumpkin seed cake was then suspended in an alkali solution at pH 11.00, which was set by 1 M NaOH. After 30 min of gentle stirring, the slurry was filtered. The proteins dissolved in the filtrate were precipitated by adjusting the pH to 4.00 with 1 M HCl. The precipitate was then separated from the liquid phase *via* centrifugation at 4 °C and 5000 rpm for 30 min. The sediment was washed with DD water until neutral and then separated by centrifugation and freeze-dried in a lyophilizer. Then, the PSPI was placed into an −80 °C refrigerator for further analysis. The protein content of the PSPI was detected as 88.96 ± 1.10% (Kjeldahl Nitrogen method, n = 3).

2.3. High-intensity ultrasonic treatment

Similar to the above method, the defatted pumpkin seed cake was suspended in an alkali solution at pH 11.0, which was adjusted by 1 M NaOH. The slurry was filtered after 30 min of gentle stirring. The dissolved proteins were ultrasonicated (ultrasonic processor, with 0.6 cm diameter titanium probe, NingBo Scientz Biotechnology Co. Ltd., Ningbo, China) at a frequency of 20 kHz. Then, an ice-water bath was applied to dissipate the heat produced during sonication. The samples were treated at 20 kHz at 100 W, 300 W, or 500 W for 30 min (pulse duration of on-time, 2 s; off-time, 2 s; the ultrasound intensity was quantitatively outputted from the ultrasonic processor). The sample without the ultrasonic treatment was set as the control. After the ultrasound treatment, all samples were precipitated by adjusting the pH to 4.00 with 1 M HCl. The precipitate was then separated from the liquid phase by centrifugation at 4 °C and 5000 rpm for 30 min. The sediment was washed with DD water until neutral, separated by centrifugation, and freeze-dried in a lyophilizer. The high-intensity ultrasound-treated pumpkin-seed protein isolate (HIU-PSPI) was obtained for further analysis.

2.4. Protein stock dispersions

The stock dispersions (1 mg/mL) of PSPI and HIU-PSPI were dispersed in phosphate-buffered saline (PBS, 0.01 M, pH 7.4) by gentle stirring for 3 h, left to stand overnight, and centrifuged at 5000 rpm for 15 min at 20 °C to obtain supernatants, which were filtered through a 0.45 μm membrane filter. When required, the stock dispersions were further diluted with PBS.

2.5. Sodium dodecyl-sulfate polyacrylamide gel (SDS-PAGE) electrophoresis

SDS-PAGE electrophoresis was carried out as described in our previous study (Cao et al., 2020) with a few modifications. PSPI and HIU-PSPI samples were dissolved with a constant protein concentration (1 mg/mL) and then mixed with 5 × loading buffer. The mixtures were incubated at 90 °C for 5 min and loaded in the gel slot. The best concentration of the separation gel was set to 10% (w/v). Electrophoresis of the stacking gel and the separating gel was conducted at 80 V and 120 V, respectively. The gel was stained with 0.1% Coomassie Brilliant Blue R-250 dye for 30 min followed by destaining in a solution containing 25% methanol and 8% acetic acid until the proper color density level was achieved. The markers of proteins (10–250 kDa) were also run in parallel on the same gel to determine the molecular weights of the proteins. Afterwards, the gel was observed and photographed.

2.6. Ultraviolet–visible (UV–Vis) spectroscopy

Using a spectrophotometer (SHIMADZU UV-1750, Japan), the UV–Vis spectra of the sample solutions (PSPI and HIU-PSPI lyophilized and prepared at a concentration of 1 mg/mL in distilled water) were recorded from 220 to 500 nm at 25 °C with a 1 cm path-length quartz cell.

2.7. Fluorescence measurement

A luminescence spectrometer (F-4600, Japan) was used to detect the fluorescence of the PSPI and HIU-PSPI solutions (0.2 mg/mL, 10 mM PBS, pH 7.4). The excitation wavelength was 290 nm, and the emission spectra ranged from 300 to 460 nm. The slit width and scan speed were 2.5 nm and 1200 nm/min, respectively.

2.8. Circular dichroism

The PSPI samples were equilibrated using a phosphate buffer (PBS, pH = 7.4, 0.01 M) and then centrifuged at 6000 r/min for 20 min. Next, supernatant containing PSPI at a concentration of 0.1 mg/mL was obtained. The second structure of PSPI was then carried out using a circular dichroism spectrometer (J-1500, JASCO Corporation, Japan) with a 0.1 cm quartz CD cuvette in a wavelength range of 185–200 nm.

2.9. Rheological behavior analysis

The rheological behavior of the PSPI samples subjected to different high-intensity ultrasound treatments was analyzed using a rheometer (AR2000ex, TA Instrument, Newcastle, Delaware, USA). The PSPI samples were equilibrated using the phosphate buffer (PBS, pH = 7.4, 0.01 M) and centrifuged at 6000 r/min for 20 min to obtain supernatant with a PSPI concentration of 0.1 mg/mL. Measurements were carried out on a 40 mm parallel plate with a gap of 1 mm. The shear-stress–-shear-rate curve was recorded using an angular frequency scanning range of 1–100 s^{-1} at a rate of 1 s^{-1} with a temperature at 25 °C. The power-law model was used to describe the flow characteristics of the PSPI system.

2.10. Sulfhydryl (-SH) content

A mixture containing 3.6 mL 20 mM Tris-hydrochloric acid buffer (containing 12% sodium dodecyl sulfate, 10 mM EDTA and 8 M urea, pH = 6.8), 0.4 mL Ellman solution (0.1% 5,5′-dithiobis-(2-nitrobenzoic acid), DTNB dissolved in 0.2 M Tris-hydrochloric acid buffer, pH = 6.8), and 5.5 mL protein solution was placed under a temperature of 40 °C for 25 min. The absorbance of the sample solution was then measured at 412 nm. The content of sulfhydryl was calculated using the molar extinction coefficient of 13,600 M^{-1} L cm^{-1}.

2.11. Surface hydrophobicity (H_0) determination

The surface hydrophobicity of the sample was detected with a fluorescence spectrum assay (SHIMADZU RF-5310PC) using 8-anilino-1-naphthalenesulfonicacid (ANSA) as a fluorescent probe (Liu et al., 2017). The 10 mL protein solution (1 mg/mL, 10 mM PBS, pH 7.4) was mixed with 0.1 mL ANSA solution (2.4 mM, 10 mM PBS, pH 7.4). The excitation wavelength was 390 nm. The emission and excitation slits were 5 nm, and the emission spectrum was measured from 400 to 650 nm. The relative exposed hydrophobicity was calculated according to Eq. (1):

$$H_0 = S_1 - S_2 \tag{1}$$

where S_1 is the area of the sample solution, and S_2 is the area of the solvent.

2.12. Quantitative color measurement

The color was determined with a colorimeter (Shang Guang WSC-S, Shanghai, China) and measured in three different places on both sides of each sample. The L* (Brightness), a^* (redness–greenness), and b^* (yellowness–blueness) values were recorded. The whiteness (W) value was calculated using Eq. (2) (PARK, 1995):

$$W = 100 - \sqrt{(100 - L^*)^2 + a^{*2} + b^{*2}}. \tag{2}$$

2.13. Determination of turbidity

Based on the method by Malik et al. (Malik et al., 2017), the protein solution was stirred for 60 min at 25 °C, and then the adsorption value was measured at 600 nm with Eppendorf BioSpectrometer fluorescence (Eppendorf Co., German).

2.14. Foaming properties and foaming microstructure observations

The foaming properties were determined according to the previously reported method with slight modifications (Resendiz-Vazquez et al., 2017; Xiong et al., 2018). Briefly, protein suspensions (10 mg/mL) of pH 4.0, 6.0, 8.0, 10.0, and 12.0 were whipped at 8000 rpm for 1 min *via* a high-shear dispersion homogenizer (JRJ300-S, Shanghai Specimen Model Factory, Shanghai, China) to produce foam. After whipping, the foam was immediately poured into a 10 mL graduated cylinder. Foaming capacity (FC) was determined by comparing the foam volume at 2 min with the initial liquid volume of the sample. The foam stability (FS) was measured by comparing the foam volume at 20 min with the initial foam volume. The microstructure of the bubbles was observed with a stereo microscope instrument (Stemi 508, Carl Zeiss, Germany). The samples (10 μL) were placed on glass microscope slides with cover slips. The foam was then observed after being stored at 25 °C for 2 and 20 min. The magnification of the microscope was 50-fold. The FC and FS values were calculated as follows:

$$FC(\%) = V_0/25 \times 100 \tag{3}$$

$$FS(\%) = V_1/V_0 \times 100 \tag{4}$$

where V_0 represents the volume of foam at 2 min, and V_1 represents the volume of foam at 20 min.

2.14.1. Scanning electron microscope (SEM)

The surface morphology of the freeze-dried PSPI samples was observed using a SEM (JEOL, JSM-6390LV, Japan) at an accelerating voltage of 20 kV. Before using the SEM, the samples were coated with gold using an ion sputter coater.

2.15. Statistical analysis

All experimental data were analyzed *via* analysis of variance (ANOVA) with a 95% confidence interval. The ANOVA data with $p < 0.05$ were considered statistically significant. All treatments were carried out in triplicate, and the results are expressed as the mean ± SD (n = 3). Statistical analysis was performed using the SPSS software, version 19.0.

3. Results and discussion

3.1. SDS-PAGE analysis

The electrophoresis profiles of the untreated and high-intensity-ultrasound treated PSPI are shown in Fig. 1. In all samples, four main bands were observed, with molecular weights of 17.2 kDa, 18.0 kDa, 36.0 kDa, and 54.3 kDa. Compared with the control, the ultrasound-treated PSPI samples did not show significant changes in their protein electrophoresis profiles, indicating that ultrasound treatment did not change the molecular weight of the PSPI. However, after 500 W high-intensity ultrasound treatment, the main protein bands became lighter in color, which means that the protein contents at this molecular weight were reduced. Xiong et al. also reported that there were no changes in the molecular weight profiles of pea protein after HIU treatment, indicating that the ultrasound treatment did not change the protein's primary structure (Xiong et al., 2018).

3.2. Ultraviolet–visible (UV) spectra

The UV–visible spectra of the control and ultrasound-treated PSPI are illustrated in Fig. 2. There were two characteristic absorption peaks of PSPI observed at 202 and 280 nm, respectively. The strong absorption

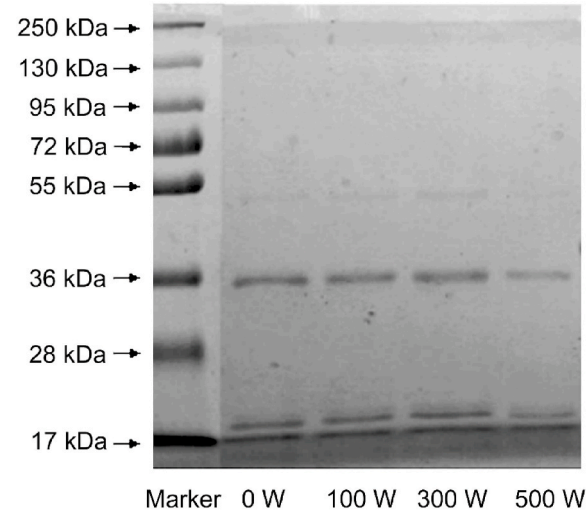

Fig. 1. SDS-PAGE profiles of pumpkin-seed protein isolates under different high-intensity ultrasound treatment conditions.

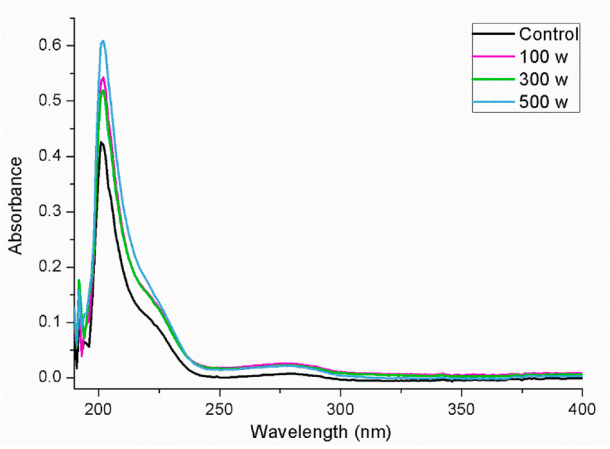

Fig. 2. Ultraviolet absorption spectra of non-HIU and HIU-treated PSPI solutions.

peak at 202 nm was mainly due to the contribution of the peptide bond, while the slight absorption peak at 280 nm was caused by chromophores such as tryptophan (Trp) and tyrosine (Try) residues (Grimsley & Pace, 2004; Ren et al., 2018). Obviously, the absorption intensity of the samples at 202 nm was enhanced with an increase in ultrasonic intensity. After the HIU treatment, the absorbance intensity of the PSPI was strengthened, indicating that more buried hydrophobic groups were transferred to the surface of the protein. Similar findings for rice protein were reported by Xue et al. (Yang et al., 2017). The UV–visible absorption maximum showed a slight right shift under different frequencies after HIU treatment. This right shift could be explained by greater unfolding of the peptide chain, which strengthened the intermolecular forces and changed the conformation of protein after ultrasonic treatment.

3.3. Fluorescence spectroscopy

Fluorescence spectra provide a sensitive means of characterizing proteins and their conformations. Tryptophan (Trp), tyrosine (Tyr), and phenylalanine (Phe) residues emit fluorescence in a manner strictly dependent on the folding of the protein, so these residues play an important role in monitoring tertiary-structure changes in protein (Jin et al., 2015). The fluorescence spectra of the samples treated with HIU under different ultrasonic powers and the control are outlined in Fig. 3. Clearly, HIU treatment was able to induce obvious changes to the tertiary structure of PSPI, as shown by changes in the maximum wave length (λ_{max}) and fluorescence intensity. The fluorescence spectra showed a slight right shift, with λ_{max} shifting from 328.2 to 329.2 nm under different intensities of HIU treatments. This right shift indicated that the polarity in the microenvironment was enhanced due to the movement of Trp residues towards the outer side of the protein molecule during the protein unfolding proces induced by the HIU treatment (Miriani et al., 2011). The fluorescence intensity of ultrasonic-treated PSPI was significantly lower than that of the control, which was attributed to the degree of protein unfolding. HIU treatment induced protein unfolding, which led to more chromophores being exposed to the solvent. This exposure increased the reduction of fluorescence intensity (Zhang et al., 2014). Similar observations were reported for a sunflower protein isolate after ultrasound treatment (Malik & Saini, 2018).

3.4. CD spectra

CD spectroscopy was used to determine the changes in the secondary structures of the proteins, including the α-helix, β-sheet, β-turns, and random coils, which have characteristic CD spectra (de Figueiredo Furtado et al., 2017). As presented in Fig. 4, changes to the secondary structural elements of PSPI and HIU-PSPI were detected by far ultraviolet (190–250 nm) of the CD spectra. The α-helix configuration showed an obvious positive band at 190 nm and two negative peaks in the range of 200–240 nm (Park et al., 2008). Contents of the secondary structure of PSPI in the treated or un-untreated HIU were calculated using the Jasco 32 software. The total contents of the secondary structure were 38.20%, 41.10%, 40.90%, and 85.00% for the control and different ultrasonic powers of 100, 300, and 500 W, respectively. Overall, the total amount of α-helix increased after HIU treatment, especially after high-ultrasonic-intensity treatment (500 W), which was consistent with a previous study (Chandrapala et al., 2010). The authors also found that the α-helix content of whey protein was significantly increased after HIU treatment.

3.5. Shear-stress flow behavior

The rheological behaviors of the PSPIs subjected to different HIU treatments are illustrated as the shear-stress–shear-rate curve in Fig. 5. The shear stress of the PSPIs gradually increased following an increase in the shear rate. A decreasing trend for the shear stress in the PSPIs was observed after HIU treatment. The parameters of the rheological data were mathematically fitted with a power-law model, and the

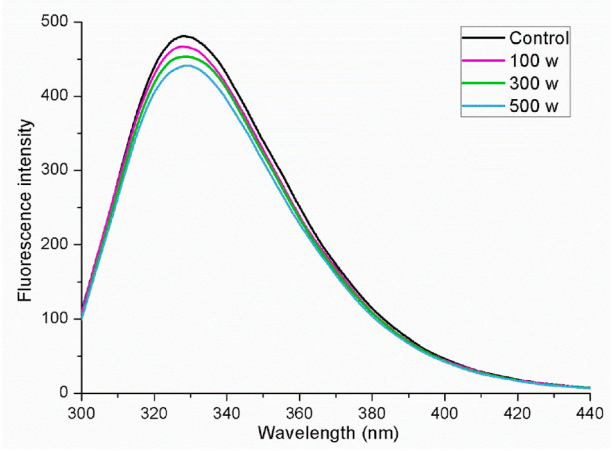

Fig. 3. Fluorescence Spectra of non-HIU and HIU-treated PSPI solutions.

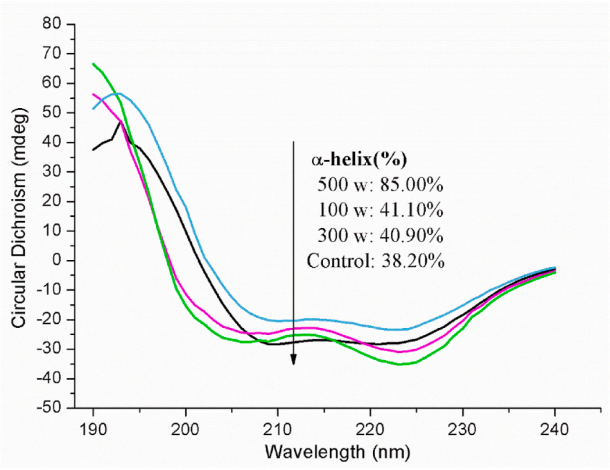

Fig. 4. CD spectra of non-HIU and HIU-treated PSPI solutions.

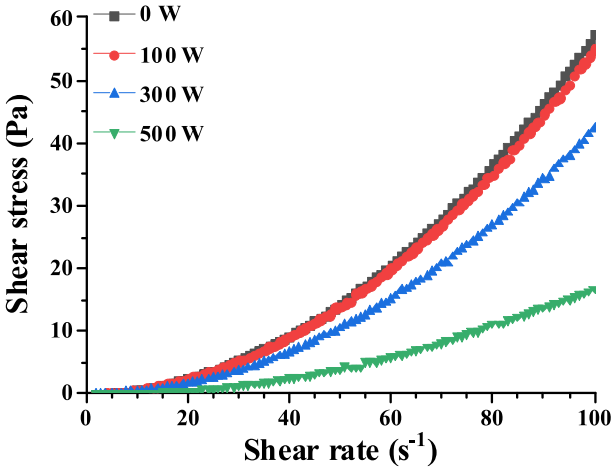

Fig. 5. Rheological behavior of non-HIU and HIU-treated PSPI solutions.

corresponding results are shown in Table 1. With an increase in the intensity of UIC, the n values related to the flow behavior index were found to be higher than 1, indicating that the PSPI solutions belonged to the dilatant fluid. K was used to represent the flow viscosity coefficient and showed an obvious decreasing trend, which suggested that the HIU treatment could improve the fluidity of PSPI and reduce its apparent viscosity.

3.6. Sulfhydryl (-SH) content

The sulfhydryl (-SH) group is an important active group in the tertiary conformational changes of protein. As shown in Fig. 6, the contents of total and reactive SH groups for PSPI and HIU-PSPI were investigated. With an increase in ultrasonic power, the content of the reactive sulfhydryl group decreased significantly, whereas the content of the total sulfhydryl group showed a slightly upward trend, especially after 500 W

Table 1
Parameters of the rheological behavior of PSPIs subjected to different HIU treatments fitted with the power law function.

HIU power	*n*	*K* (mPa·s)	R^2
0 W	1.9903	5.97	0.999986
100 W	1.9694	6.31	0.999974
300 W	2.0177	3.89	0.999969
500 W	2.0779	1.19	0.999622

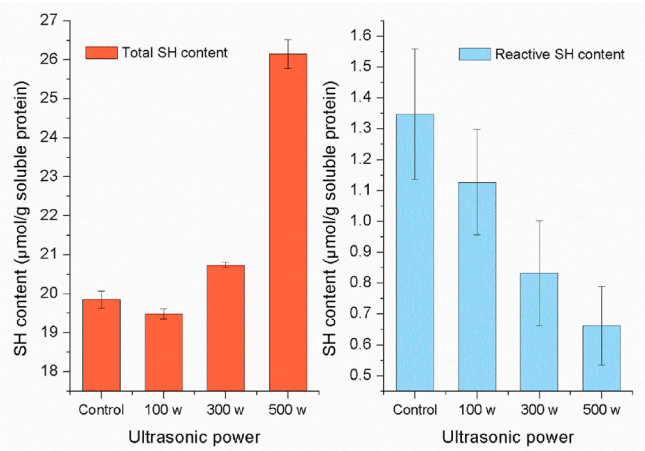

Fig. 6. Changes in the contents of total SH groups (A) and reactive SH groups (B) of non-HIU and HIU-treated PSPI solutions (mean ± SD, n = 3).

HIU treatment. These results occurred because some transition radicals produced by the ultrasonic cavitation effect can restructure hydrogen peroxide, which oxidizes with reactive SH causing the corresponding content to decrease (Gülseren et al., 2007). Similar findings were reported in previous studies on soybean protein isolate after HIU treatment (Hao et al., 2013). After high-intensity ultrasound treatment, due to the destruction of the disulfide bond of the protein and the cavitation effect, the amount of SH exposed on the surface of the PSPI increased significantly. Therefore, the content of total sulfhydryl in the PSPI increased significantly as the ultrasonic power increased, which further demonstrated the partial expansion in the molecular structure of the protein.

3.7. Surface hydrophobicity (H_0)

Surface hydrophobicity is another key index of protein's tertiary structure and hydrophobic interactions and is closely associated with protein's functional properties. As shown in Fig. 7A, the surface hydrophobicity of the ultrasound-treated PSPI was significantly increased compared to the control ($p < 0.05$). This phenomenon could be attributed to the turbulence caused by ultrasonic cavitation and physical shearing, which led to the unfolding of protein molecules and the exposure of hydrophobic amino acid residues hidden inside the protein molecule, as previously shown (Jiang et al., 2017; Resendiz-Vazquez et al., 2017). This result also agrees with the results for soy protein after ultrasound treatment, which presented remarkable enhancement of the H_0 value under different ultrasonic-power treatments (Hao et al., 2013).

3.8. Determination of turbidity

The turbidity of a protein solution is related to the protein's particle size and structure. The turbidity of the samples was quantified as a percentage of transmitted light measured at 600 nm (%T 600 nm). Fig. 7B illustrates a turbidity histogram of the PSPI solution affected by HIU treatment. As shown in the figure, the turbidity of the protein solution was significantly decreased after ultrasonic treatment. Following an increase in ultrasonic power, the turbidity of the PSPI solution was decreased. The turbidity of the protein solution was associated closely with particle light scattering: the smaller the particle size of the protein, the less likely light scattering was to form. The small particles obtained after HIU treatment resulted in decreased turbidity in the PSPI solution. Zisu et al. (Zisu et al., 2011) showed that a decreased turbidity value was caused by particle-size reduction after ultrasonic treatment, which is consistent with the results of this study.

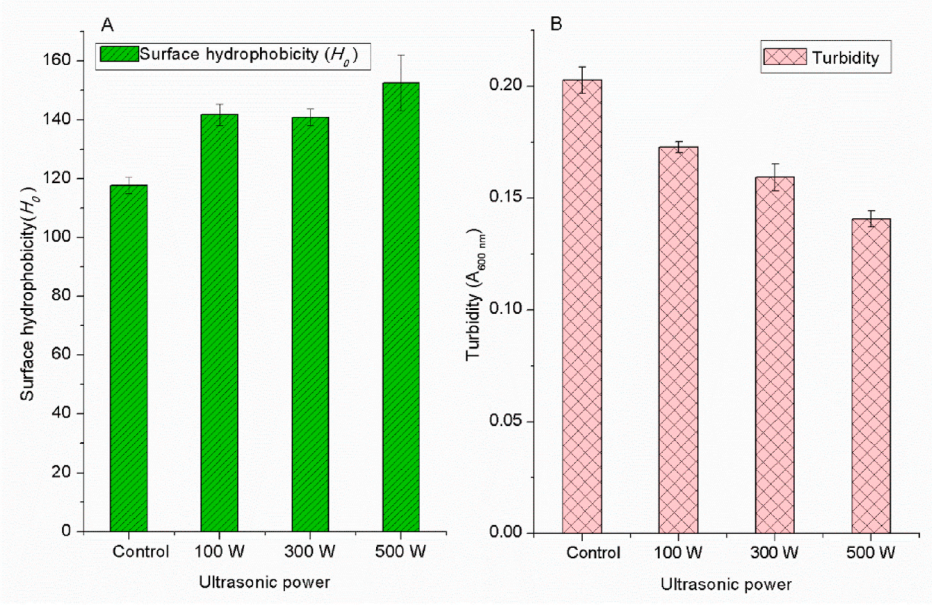

Fig. 7. Changes in the surface hydrophobicity (H_0) (A) and turbidity (B) of non-HIU and HIU-treated PSPI solutions (mean ± SD, n = 3).

3.9. Quantitative color measurement

The ultrasonic cavitation effect induced by HIU modified the structure of the protein and resulted in an increase in the number of chromophoric groups exposed to the solvent and thus affecting the chroma index of the protein. Table 2 illustrates the changes in chromaticity of the PSPI under different HIU treatments. The results showed that with an increase in ultrasonic power, higher L^* values were obtained. When the ultrasonic power was 500 W, the difference was apparent ($p < 0.05$) compared to the value of L^*. The ultrasound-treated PSPI was also lighter than native PSPI. HIU treatments had negative effects on the a^* and b^* values of the PSPI solution, which means that the PSPIs treated with HIU were inclined to be greener and less yellow. Based on the different analyses of the values of L^*, a^*, and b^*, the chromaticity of the samples changed greatly, showing significant differences with an ultrasonic power of 500 W ($p < 0.05$). Flores-Jiménez et al. reported that the HIU treatment of canola protein isolate increased the L^* value and decreased the values of a^* and b^*, which are similar to our results (Flores-Jiménez et al., 2019).

3.10. Foaming properties

Fig. 8 presents the foaming capacity (FC) and foaming stability (FS) of the PSPI, both before and after ultrasonic treatment at different pH values and under different high-intensity ultrasonic treatment conditions. In general, both the FC and FS values were changed under different pH conditions, with overall upward trends. The FC (%) values of the pumpkin-seed protein isolates were significantly increased after high-intensity ultrasound treatment. Compared to the untreated PSPI (control), the FC values of the HIU-PSPI were about two-fold higher than those of the control at the same pH values. The results indicated that high-intensity ultrasonic treatment could promote the foaming ability of PSPI, which is consistent with many previous reports. For example, Morales et al. evaluated the effects of high-intensity ultrasonic treatment (20 kHz, 150 W) on the foaming performance of soybean protein after 20 min, showing that the FC value was significantly increased (Morales et al., 2015). Similar results were obtained by Xiong et al. (2016), who showed that the FC values of egg albumin extracted from egg whites improved after HIU treatment (Xiong et al., 2016). In Fig. 8, the changes in FS (%) indicate a downward trend under different ultrasound powers (100, 300, and 500 W) after treatment for 20 min at pH values of 4.0–8.0. However, the changes in FS (%) gradually increased from pH 8.0 to 12.0, indicating an increase in foam stability. This primarily occurred because more hydrophobic groups and regions were exposed to the surface during ultrasonic treatment, which induced an increase in protein aggregation, thereby reducing protein activity, which resulted in a decrease of the corresponding FS values. The increase in H_0 values (Fig. 7A) was also responsible for improving the foam's capacity and stability due to the exposure of hydrophobic groups to accelerated adsorption at the gas/water interface (Delahaije et al., 2014). At the same time, the increase of FC in the PSPI was due to changes in protein conformation (Fig. 4), which made the protein flexible and loose, leading to the production of more foam.

Table 2
Effect of different high-intensity ultrasound treatment conditions on the chromaticity of non-HIU and HIU-treated PSPIs (mean ± SD, n = 3).

HIU power	L^*	a^*	b^*
0 W	56.7250 ± 0.43949b	−0.6167 ± 0.02422b	0.8933 ± 0.05955b
100 W	56.8650 ± 0.13342b	−0.6200 ± 0.09852 ab	0.8612 ± 0.04324 ab
300 W	56.8825 ± 0.40447b	−0.6000 ± 0.02330 ab	0.6987 ± 0.04016 ab
500 W	58.1725 ± 0.50048a	−0.6300 ± 0.01309a	0.8288 ± 0.08288a

Different small letters within the same row represent significant differences (P < 0.05) between groups.

3.11. Microstructure observations of foaming

To investigate the morphology of the PSPI foams, the microstructures were analyzed using a stereo microscope, and the results are shown in Fig. 9. In general, compared to the control, the foam produced by HIU-PSPI produced larger-sized bubbles that were more evenly distributed during the first 2 min, which is especially clear in the image showing an ultrasonic power of 500 W. The results showed that the foaming performance of the PSPI treated with ultrasound was not significantly better than that of the untreated PSPI. With an increase in time from 2 to 20 min, the bubble size of the PSPI gradually increased, largely because aqueous foam systems are unbalanced, which induced gravity drainage,

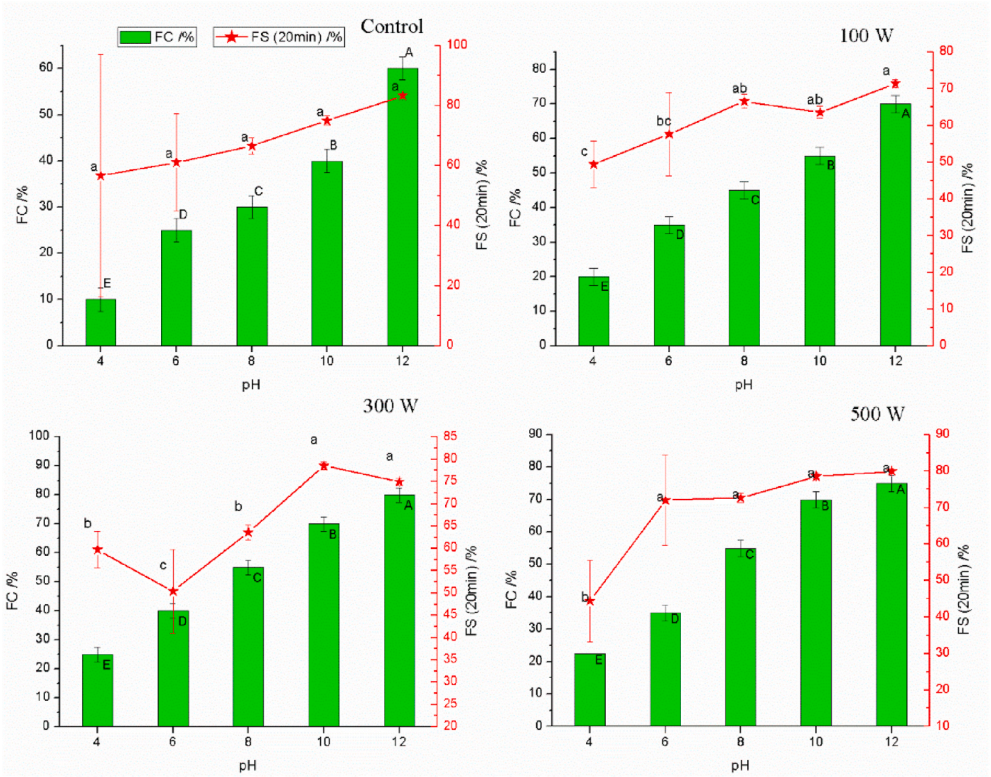

Fig. 8. Changes in the foaming capacity (FC) and foaming stability (FS) of non-HIU and HIU-treated PSPI solutions under different HIU powers at different pH values (mean ± SD, n = 3). Different superscript letters mean significant differences between values with different ultrasonic powers ($p < 0.05$).

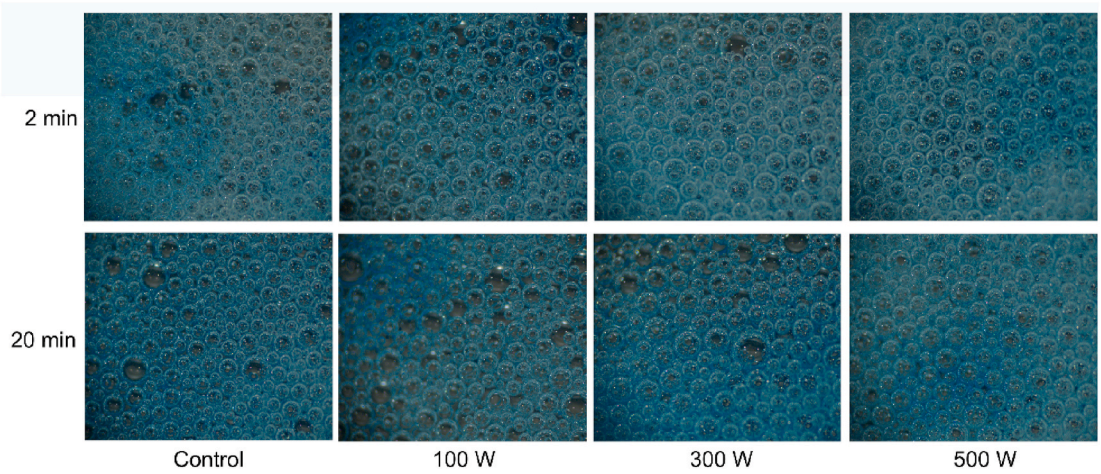

Fig. 9. Time evolution of bubble formation in the pumpkin-seed protein-isolate solution under different high-intensity ultrasound treatment conditions.

coarsening, foam rupture, and bubble growth, which eventually increased the average bubble size (Saint-Jalmes & Langevin, 2002). Compared with untreated pumpkin-seed protein isolates, the bubbles produced after ultrasound treatment for 20 min showed larger-diameter bubbles as the ultrasonic power increased. The microstructures of the PSPI foams treated with ultrasounds at different frequencies were similar.

3.12. Scanning electron microscopy (SEM)

To understand the effects of different ultrasonic treatments on the PSPI, the microstructure of the lyophilized PSPI was observed by SEM. Fig. 10 presents SEM images of the PSPI samples obtained at 150× magnification under different ultrasonic-power treatments (100, 300, and 500 W) and the control. As shown in Fig. 10, compared to the compact structure of the control, the morphologies of the samples treated with different ultrasonic powers became loose and were accompanied by irregular small debris. In addition, with an increase in ultrasonic processing power, the fragments became smaller and more regular and expanded their distribution. These microstructural changes might be due to the expansion of protein molecules induced by increased exposure of the hydrophobic groups and free-SH groups embedded in the molecule (Malik & Saini, 2018; Xiong et al., 2018), which could change the surface hydrophobicity and interaction forces (such as electrostatic effects) (He et al., 2021), resulting in the formation of irregular fragments. These results are consistent with the

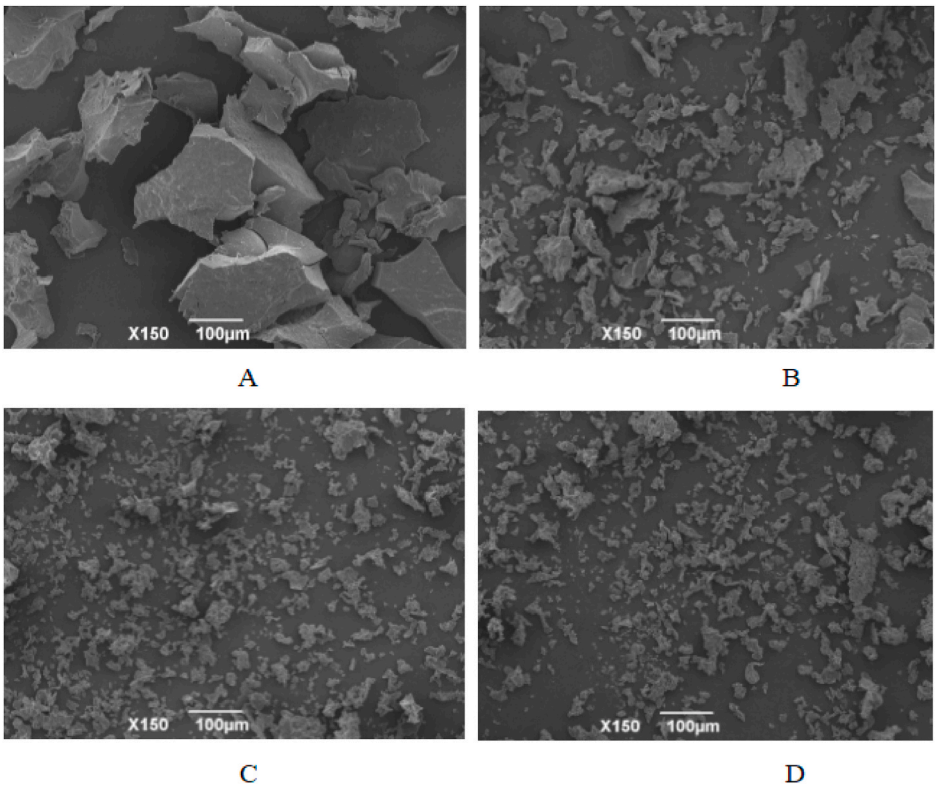

Fig. 10. Scanning electron microscopy (SEM) of freeze-dried PSPI powder under treatments with different ultrasonic powers: A) control, B) 100 W, C) 300 W, D) 500 W.

microstructures of protein isolates extracted from the pea (Xiong et al., 2018) and whey protein (Khatkar et al., 2018) under HIU treatments. Moreover, the ultrasound effect can lead to the destruction of the protein's molecular structure, a decrease in particle size, the dispersion of protein aggregation, and the formation of a more loose structure after lyophilization (Shukla et al., 2019). These results indicate that the surface microstructure of the HIU-PSPI after ultrasound treatment changed significantly compared to the control.

4. Conclusions

Based on the results of this study, HIU is an effective technique for improving the physicochemical and functional properties of pumpkin-seed protein isolates. Compared with the control, ultrasound processing caused partial unfolding of the PSPIs, leading to secondary and tertiary structural changes that were observed by CD, UV–visible spectroscopy, and surface hydrophobicity. Furthermore, scanning electron microscopy showed that high-intensity ultrasonic treatment yielded a more disordered structure and the appearance of irregular small pieces. With an increase in ultrasonic power, the brightness significantly increased, and the turbidity significantly decreased. Moreover, the foaming capability and stability of the PSPIs improved significantly after HIU treatments. These physicochemical and structural changes that occurred in the pumpkin-seed protein isolates meet the complex requirements of food processing varieties. Therefore, ultrasound is an effective technology that could be used in the food industry to improve the functional properties of plant proteins.

Data availability statement

The datasets in the present study are available from the corresponding author upon reasonable request.

CRediT authorship contribution statement

Hongying Du: Conceptualization, Investigation, Formal analysis, Funding acquisition, Writing – original draft. **Jin Zhang:** Formal analysis, Investigation, Project administration. **Siqi Wang:** Formal analysis, Investigation, Project administration. **Anne Manyande:** Writing – review & editing. **Jie Wang:** Conceptualization, Investigation, Writing – review & editing.

Declaration of competing interest

The authors report no conflicts of interest.

Acknowledgements

This research was financially supported by the National Natural Science Foundation of China (No. 31772047), the Fundamental Research Funds for the Central Universities in China (No. 2662019PY031), Youth Innovation Promotion Association of Chinese Academy of Sciences (No. Y6Y0021004), and Young Professionals Promotion Funds of Zhejiang Academy of Agricultural Sciences (No. 2020R15R08E01).

References

Aktaş, N., Uzlaşır, T., & Tunçil, Y. E. (2018). Pre-roasting treatments significantly impact thermal and kinetic characteristics of pumpkin seed oil. *Thermochimica Acta, 669*, 109–115.

Bučko, S., Katona, J., Petrović, L., Milinković, J., Spasojević, L., Mucić, N., & Miller, R. (2018). The influence of enzymatic hydrolysis on adsorption and interfacial dilatational properties of pumpkin (cucurbita pepo) seed protein isolate. *Food Biophysics, 13*, 217–225.

Bučko, S., Katona, J., Popović, L., Petrović, L., & Milinković, J. (2016). Influence of enzymatic hydrolysis on solubility, interfacial and emulsifying properties of pumpkin (Cucurbita pepo) seed protein isolate. *Food Hydrocolloids, 60*, 271–278.

Bučko, S., Katona, J., Popović, L., Vaštag, Ž., Petrović, L., & Vučinić–Vasić, M. (2015). Investigation on solubility, interfacial and emulsifying properties of pumpkin

(Cucurbita pepo) seed protein isolate. *Lebensmittel-Wissenschaft und -Technologie-Food Science and Technology, 64*, 609–615.
Cao, Q., Huang, Y., Zhu, Q.-F., Song, M., Xiong, S., Manyande, A., & Du, H. (2020). The mechanism of chlorogenic acid inhibits lipid oxidation: An investigation using multi-spectroscopic methods and molecular docking. *Food Chemistry, 333*, Article 127528.
Chandrapala, J., Zisu, B., Palmer, M., Kentish, S., & Ashokkumar, M. (2010). Effects of ultrasound on the thermal and structural characteristics of proteins in reconstituted whey protein concentrate. *Ultrasonics Sonochemistry, 18*, 951–957.
Chemat, F., Zill e, H., & Khan, M. K. (2011). Applications of ultrasound in food technology: Processing, preservation and extraction. *Ultrasonics Sonochemistry, 18*, 813–835.
Delahaije, R. J. B. M., Gruppen, H., Giuseppin, M. L. F., & Wierenga, P. A. (2014). Quantitative description of the parameters affecting the adsorption behaviour of globular proteins. *Colloids and Surfaces B: Biointerfaces, 123*, 199–206.
de Figueiredo Furtado, G., Mantovani, R. A., Consoli, L., Hubinger, M. D., & da Cunha, R. L. (2017). Structural and emulsifying properties of sodium caseinate and lactoferrin influenced by ultrasound process. *Food Hydrocolloids, 63*, 178–188.
Flores-Jiménez, N. T., Ulloa, J. A., Silvas, J. E. U., Ramírez, J. C. R., Ulloa, P. R., Rosales, P. U. B., Carrillo, Y. S., & Leyva, R. G. (2019). Effect of high-intensity ultrasound on the compositional, physicochemical, biochemical, functional and structural properties of canola (Brassica napus L.) protein isolate. *Food Research International, 121*, 947–956.
Grimsley, G. R., & Pace, C. N. (2004). Spectrophotometric determination of protein concentration. *Current Protocols in Protein Science, 33*, 3. 1.1-3.1.9.
Gülseren, İ., Güzey, D., Bruce, B. D., & Weiss, J. (2007). Structural and functional changes in ultrasonicated bovine serum albumin solutions. *Ultrasonics Sonochemistry, 14*, 173–183.
Hao, H., Wu, J., Li-Chan, E. C. Y., Zhu, L., Zhang, F., Xu, X., Fan, G., Wang, L., Huang, X., & Pan, S. (2013). Effects of ultrasound on structural and physical properties of soy protein isolate (SPI) dispersions. *Food Hydrocolloids, 30*, 647–655.
He, X., Chen, J., He, X., Feng, Z., Li, C., Liu, W., Dai, T., & Liu, C. (2021). Industry-scale microfluidization as a potential technique to improve solubility and modify structure of pea protein. *Innovative Food Science & Emerging Technologies, 67*, Article 102582.
Jiang, S., Ding, J., Andrade, J., Rababah, T. M., Almajwal, A., Abulmeaty, M. M., & Feng, H. (2017). Modifying the physicochemical properties of pea protein by pH-shifting and ultrasound combined treatments. *Ultrasonics Sonochemistry, 38*, 835–842.
Jin, J., Ma, H., Wang, K., Yagoub, A. E.-G. A., Owusu, J., Qu, W., He, R., Zhou, C., & Ye, X. (2015). Effects of multi-frequency power ultrasound on the enzymolysis and structural characteristics of corn gluten meal. *Ultrasonics Sonochemistry, 24*, 55–64.
Khatkar, A. B., Kaur, A., Khatkar, S. K., & Mehta, N. (2018). Characterization of heat-stable whey protein: Impact of ultrasound on rheological, thermal, structural and morphological properties. *Ultrasonics Sonochemistry, 49*, 333–342.
Liu, R., Liu, Q., Xiong, S., Fu, Y., & Chen, L. (2017). Effects of high intensity unltrasound on structural and physicochemical properties of myosin from silver carp. *Ultrasonics Sonochemistry, 37*, 150–157.
Malik, M. A., & Saini, C. S. (2018). Rheological and structural properties of protein isolates extracted from dephenolized sunflower meal: Effect of high intensity ultrasound. *Food Hydrocolloids, 81*, 229–241.
Malik, M. A., Sharma, H. K., & Saini, C. S. (2017). High intensity ultrasound treatment of protein isolate extracted from dephenolized sunflower meal: Effect on physicochemical and functional properties. *Ultrasonics Sonochemistry, 39*, 511–519.
Martínez-Velasco, A., Lobato-Calleros, C., Hernández-Rodríguez, B. E., Román-Guerrero, A., Alvarez-Ramirez, J., & Vernon-Carter, E. J. (2018). High intensity ultrasound treatment of faba bean (Vicia faba L.) protein: Effect on surface properties, foaming ability and structural changes. *Ultrasonics Sonochemistry, 44*, 97–105.
Miriani, M., Keerati-u-rai, M., Corredig, M., Iametti, S., & Bonomi, F. (2011). Denaturation of soy proteins in solution and at the oil–water interface: A fluorescence study. *Food Hydrocolloids, 25*, 620–626.
Mir, N. A., Riar, C. S., & Singh, S. (2019). Physicochemical, molecular and thermal properties of high-intensity ultrasound (HIUS) treated protein isolates from album (Chenopodium album) seed. *Food Hydrocolloids, 96*, 433–441.
Mitić, M., Pavlović, A., Tošić, S., Mašković, P., Kostić, D., Mitić, S., Kocić, G., & Mašković, J. (2018). Optimization of simultaneous determination of metals in commercial pumpkin seed oils using inductively coupled atomic emission spectrometry. *Microchemical Journal, 141*, 197–203.
Morales, R., Martínez, K. D., Pizones Ruiz-Henestrosa, V. M., & Pilosof, A. M. R. (2015). Modification of foaming properties of soy protein isolate by high ultrasound intensity: Particle size effect. *Ultrasonics Sonochemistry, 26*, 48–55.
Nkosi, C. Z., Opoku, A. R., & Terblanche, S. E. (2006). In Vitro antioxidative activity of pumpkin seed (Cucurbita pepo) protein isolate and its in Vivo effect on alanine transaminase and aspartate transaminase in acetaminophen-induced liver injury in low protein fed rats. *Phytotherapy Research, 20*, 780–783.
Ojha, K. S., Aznar, R., O'Donnell, C., & Tiwari, B. K. (2020). Ultrasound technology for the extraction of biologically active molecules from plant, animal and marine sources. *TRAC Trends in Analytical Chemistry, 122*, Article 115663.
Park, J. W. (1995). Surimi gel colors as affected by moisture content and physical conditions. *Journal of Food Science, 60*, 15–18.
Park, K., Perczel, A., & Fasman, G. D. (2008). Differentiation between transmembrane helices and peripheral helices by the deconvolution of circular dichroism spectra of membrane proteins. *Protein Science, 1*, 1032–1049.
Quirino, D., Yufei, H., Kingsley, G. M., & Caimeng, Z. (2014). Effect of Xanthan and Arabic gums on foaming properties of pumpkin (cucurbita pepo) seed protein isolate. *Journal of Food Research, 3*, 87–95.
Ren, C., Xiong, W., Peng, D., He, Y., Zhou, P., Li, J., & Li, B. (2018). Effects of thermal sterilization on soy protein isolate/polyphenol complexes: Aspects of structure, in vitro digestibility and antioxidant activity. *Food Research International, 112*, 284–290.
Resendiz-Vazquez, J. A., Ulloa, J. A., Urías-Silvas, J. E., Bautista-Rosales, P. U., Ramírez-Ramírez, J. C., Rosas-Ulloa, P., & González-Torres, L. (2017). Effect of high-intensity ultrasound on the technofunctional properties and structure of jackfruit (Artocarpus heterophyllus) seed protein isolate. *Ultrasonics Sonochemistry, 37*, 436–444.
Saint-Jalmes, A., & Langevin, D. (2002). Time evolution of aqueous foams: Drainage and coarsening. *Journal of Physics: Condensed Matter, 14*, 9397–9412.
Shukla, S., Khan, I., Bajpai, V. K., Lee, H., Kim, T., Upadhyay, A., Huh, Y. S., Han, Y.-K., & Tripathi, K. M. (2019). Sustainable graphene aerogel as an ecofriendly cell growth promoter and highly efficient adsorbent for histamine from red wine. *ACS Applied Materials & Interfaces, 11*, 18165–18177.
Téllez-Morales, J. A., Hernández-Santo, B., & Rodríguez-Miranda, J. (2020). Effect of ultrasound on the techno-functional properties of food components/ingredients: A review. *Ultrasonics Sonochemistry, 61*, Article 104787.
Wang, X., Wu, J., Yu, B., Dong, K. F., Ma, D., Xiao, G., & Zhang, C. (2020). Heavy metals in aquatic products and the health risk assessment to population in China. *Environmental Science and Pollution Research, 27*, 22708–22719.
Wen, C., Zhang, J., Zhang, H., Duan, Y., & Ma, H. (2019). Effects of divergent ultrasound pretreatment on the structure of watermelon seed protein and the antioxidant activity of its hydrolysates. *Food Chemistry, 299*, Article 125165.
Xiong, W., Wang, Y., Zhang, C., Wan, J., Shah, B. R., Pei, Y., Zhou, B., Li, J., & Li, B. (2016). High intensity ultrasound modified ovalbumin: Structure, interface and gelation properties. *Ultrasonics Sonochemistry, 31*, 302–309.
Xiong, T., Xiong, W., Ge, M., Xia, J., Li, B., & Chen, Y. (2018). Effect of high intensity ultrasound on structure and foaming properties of pea protein isolate. *Food Research International, 109*, 260–267.
Yang, X., Li, Y., Li, S., Oladejo, A. O., Ruan, S., Wang, Y., Huang, S., & Ma, H. (2017). Effects of ultrasound pretreatment with different frequencies and working modes on the enzymolysis and the structure characterization of rice protein. *Ultrasonics Sonochemistry, 38*, 19–28.
Yang, C., Wang, B., Wang, J., Xia, S., & Wu, Y. (2019). Effect of pyrogallic acid (1,2,3-benzenetriol) polyphenol-protein covalent conjugation reaction degree on structure and antioxidant properties of pumpkin (Cucurbita sp.) seed protein isolate. *Lebensmittel-Wissenschaft und -Technologie, 109*, 443–449.
Zhang, L., Pan, Z., Shen, K., Cai, X., Zheng, B., & Miao, S. (2018). Influence of ultrasound-assisted alkali treatment on the structural properties and functionalities of rice protein. *Journal of Cereal Science, 79*, 204–209.
Zhang, Q. T., Tu, Z.-C., Xiao, H., Wang, H., Huang, X.-Q., Liu, G.-X., Liu, C.-M., Shi, Y., Fan, L.-L., & Lin, D.-R. (2014). Influence of ultrasonic treatment on the structure and emulsifying properties of peanut protein isolate. *Food and Bioproducts Processing, 92*, 30–37.
Zhao, W., Shu, Q., He, G., & Qihe, C. (2020). Reducing antigenicity of bovine whey proteins by Kluyveromyces marxianus fermentation combined with ultrasound treatment. *Food Chemistry, 311*, 125893.
Zisu, B., Lee, J., Chandrapala, J., Bhaskaracharya, R., Palmer, M., Kentish, S., & Ashokkumar, M. (2011). Effect of ultrasound on the physical and functional properties of reconstituted whey protein powders. *Journal of Dairy Research, 78*, 226–232.
Zou, Y., Xu, P., Wu, H., Zhang, M., Sun, Z., Sun, C., Wang, D., Cao, J., & Xu, W. (2018). Effects of different ultrasound power on physicochemical property and functional performance of chicken actomyosin. *International Journal of Biological Macromolecules, 113*, 640–647.